Journal of ELECTRONIC MATERIALS, Vol. 45, No. 5, 2016
DOI: 10.1007/s11664-016-4372-1

Development of a PMMA Electrochemical Microfluidic Device for Carcinoembryonic Antigen Detection

NGUYEN VAN ANH,[1,6] HOANG VAN TRUNG,[2] BUI QUANG TIEN,[3] NGUYEN HAI BINH,[2] CAO HONG HA,[1] NGUYEN LE HUY,[1] NGUYEN THAI LOC,[4] VU THI THU,[3] and TRAN DAI LAM[5,7,8]

1.—Hanoi University of Science and Technology, 1, Dai Co Viet, Hai Ba Trung, Ha Noi, Vietnam. 2.—Institute of Materials Science, Vietnam Academy of Science and Technology, 18, Hoang Quoc Viet, Cau Giay, Ha Noi, Vietnam. 3.—University of Science and Technology of Hanoi, 18, Hoang Quoc Viet, Cau Giay, Ha Noi, Vietnam. 4.—Asian Institute of Technology, 58 Moo 9, Paholyothin Highway Klong Luang, Pathumthani 12120, Thailand. 5.—Graduate University of Science and Technology, Vietnam Academy of Science and Technology, 18 Hoang Quoc Viet Road, Hanoi, Vietnam. 6.—e-mail: anh.nguyenvan@hust.edu.vn. 7.—e-mail: trandailam@gmail.com. 8.—e-mail: tdlam@gust-edu.vast.vn

In this study, a poly(methyl methacrylate) (PMMA) microfluidic device fabricated by an inexpensive CO_2 laser etching system was developed for detection of carcino-embryonic antigens (CEA). The device was capable of working in continuous mode and was designed with the aid of numerical simulation. The detection of target CEA was based on immuno-assay via magnetic particles and electrochemical sensing. The as-prepared microfluidic can be used to detect CEA at the relatively low concentration of 150 pg mL^{-1}. The device could be reused many times, since the capture and removal of magnetic particles in the assay could be manipulated by an external magnetic field. The proposed approach appears to be suitable for high-throughput and automated analysis of large biomolecules such as tumor markers and pathogens.

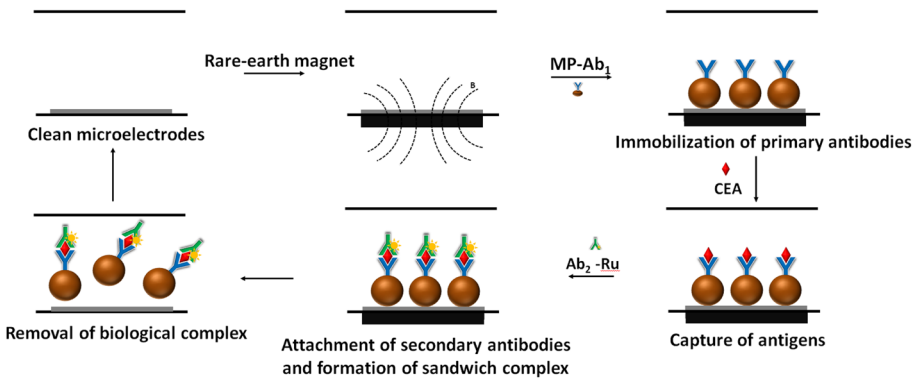

Key words: CEA, magnetic particles, continuous flow mode, immunosensor, microfluidic, automated

(Received December 18, 2015; accepted January 22, 2016; published online February 18, 2016)

INTRODUCTION

Carcino-embryonic antigens (CEA) are associated with colon, lung, ovarian, breast and many other cancers.[1] The determination of these tumor markers hence plays an important role in clinical research and diagnosis.[1–4] The CEA level in human blood can be used to diagnose cancer diseases and monitor cancer treatment. Many different methods have been developed for cancer detection. Currently, enzyme-linked immunosorbent assay (ELISA) is the most widely used diagnosis method in laboratories. However, the ELISA test suffers from many drawbacks such as time-consuming procedures, large sample volume, and limited sensitivity.[5] Electrochemical immunosensors are a viable alternative method with high sensitivity, short diagnostic time, low cost and the possibility of miniaturization.[6–12] For example, amperometric immunosensors using gold nanoparticles for CEA analysis with the detection limit up to 100 pg mL^{-1} have been reported by many research groups.[6–9] In addition, electrochemical immunosensors can be used to detect CEA markers not only in serum but also in saliva.[10] Gurbuz and coworkers have successfully developed a novel magnetic particle-modified capacitive sensor for CEA with a linear range from 5 pg mL^{-1} to 1 ng mL^{-1} and a detection limit of 20 pg.mL^{-1}.[11] On the other hand, the use of graphene and Cu@Ag Core–shell can lower the detection limit of a CEA immunosensor to as low as 20 fg mL^{-1}.[12] Despite these advantages, the application of electrochemical immunosensors remains laborious and inconvenient due to the lack of automated manipulation of biomolecules.

Evidence from several studies suggested that a fully automated analysis microsystem for biomolecules could be developed by combining an electrochemical immunosensor, magnetic separation and microfluidic flow. The load/release of biomolecules on electrode surfaces can be readily manipulated via magnetic particles under an external magnetic field gradient.[13,14] Meanwhile, the sensitivity of the analysis system can be improved by avoiding non-specific adsorption, removing unreacted reagents and increasing binding areas when target molecules binding to magnetic particles are preconcentrated on microelectrodes. Furthermore, biomolecules (enzymes, antibodies, oligonucleotides, etc.) can be easily immobilized on magnetic particles which have been functionalized with appropriate organic molecular groups such as amine, hydroxyl, carboxyl, aldehyde, thiol, biotin or streptavidin.[14] In the last two decades, microfluidics has greatly facilitated biomedical analysis by reducing the sample volume required, improving the sensitivity and detection limit, reducing assay time, and minimizing manufacturing cost, technical expertise and system maintenance.[15,16]

Several automated microsystems have been demonstrated to have excellent accuracy as compared to traditional assays. For example, Verbarg[17] used a spinning permanent magnetic trap and magnetic beads to capture, mix, and release target molecules within a microfluidic channel. Berti[18] has developed an automated electrochemical genosensor using a novel microfluidic-based platform to determine hazelnut amplicon with a detection limit of 200 pg mL^{-1}. The device can be regenerated after each assay by removing the external magnetic field. Recently, Wheeler has reported the first automated digital microfluidic platform capable of performing immunoassays in near-patient settings.[19] Clearly, microfluidic devices combined with electrochemical immunosensor form a promising candidate for the automation of biomedical analysis.

In this work, we have developed a microfluidic device for the rapid and sensitive quantification of a CEA tumor marker. The detection of CEA relied on an electrochemical immunosensor, and the capture and release of the antibodies/antigen complex was manipulated using magnetic particles. The device was optimized and tested by numerical simulation and experiment. The ability of the system to detect CEA markers was evaluated using standard samples and the detection limit was determined.

EXPERIMENTAL

Materials

Streptavidin-coated magnetic particles (0.72 mg mL^{-1}, 1 μm diameter), biotinylated monoclonal anti-CEA antibody (Ab_1-biotin, mouse/human, 3.0 mg mL^{-1}), monoclonal anti-CEA antibody labeled with ruthenium complex (Ab_2-Ru, mouse, 4.0 mg L^{-1}) and carcinoembryonic antigen (CEA) with standard concentrations were purchased from Roche (Basel, Switzerland). *Staphylococcal enterotoxin B* (SEB) was purchased from Toxin Technology (Sarasota, FL, USA). The rare-earth magnets (Neodymium, NdFeB) were purchased from a local supplier.

Fabrication of Microelectrodes

The sensor with a 3-electrode set-up was prepared on a thermally oxidized silicon wafer as described in our previous work.[20] The silicon wafer, with a 600-nm-thick silicon dioxide layer, was first spin-coated with a layer of photoresist (AZ 5214E) of 1 μm, and then the shape of the electrodes was defined by UV–photolithography. Then, chromium (Cr) and platinum (Pt) were sputtered on the top of the wafer with thicknesses of 20 and 200 nm, respectively. The platinum working electrodes (WE) and counter electrodes (CE) were patterned by a lift-off process. A second photolithographic step was carried out to pattern a silver (Ag) layer. Partial chlorination of the Ag layer, performed in 0.25 mol.L^{-1} $FeCl_3$ solution, was used as for a fabricating reference electrode (RE).

Design, Simulation and Fabrication of a PMMA Microfluidic Device

Layer-By-Layer Design

The configuration of a microfluidic device is descbribed in Fig. 1a. The system consists of 3 layers: (1) PMMA fluidic system (layer 1); (2) silicon joint (layer 2); and (3) supporting plate (layer 3). The top layer is a fluidic system containing a

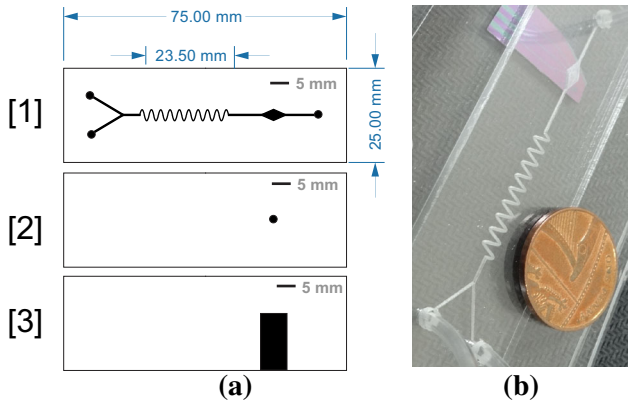

Fig. 1. PMMA microfluidic device. (a) Conceptual illustration: layer [1] PMMA fluidic platform: inlets, micromixer, reaction chamber, outlet; layer [2] silicon joint; layer [3] supporting plate with electrode fixtures; (b) actual prototype of the PMMA microfluidic device. The depth of the microchannel is 300 μm.

serpentine micromixer and a reaction chamber. At the entrance of the fluidic system, there are two inlets that will be used to inject samples and reagents. An electrochemical immunosensor with a 3-electrode set-up was prepared and inserted right under the reaction chamber. The bottom layer of the device was a supporting plate in which a rectangular hole was engraved as the electrode fixture. A middle layer of silicon was inserted between the fluidic platform and the cover plate to prevent the leakage of solutions.

Simulation

In this study, two inflow streams were mixed by a passive serpentine microchannel based on diffusion.[21] To maximize the mixing effects of the micromixer, the flow of liquids was simulated by COMSOL Multiphysics software (v.4.3) using weakly compressible Navier–Stokes flow module and the convection and diffusion module. The channel geometry used was identical to the nominal geometry used in the experiments, though there was minor certain device-to-device variation. The flow of fluids in the channels was described by the Navier–Stokes equations:

$$\rho(u \cdot \nabla)u - \nabla \cdot \eta\left(\nabla u + (\nabla u)^T\right) + \nabla p = 0 \quad (1)$$

$$\nabla \cdot u = 0 \quad (2)$$

And the convection–diffusion equation:

$$D\nabla^2 c - u \cdot \nabla c = 0 \quad (3)$$

where ρ is the fluid density (kg m^{-3}), u is the linear velocity (m s^{-1}), η denotes fluid viscosity (Pa.s), p is the pressure (Pa), D is the diffusion coefficient (m^2 s^{-1}) and c is the concentration (mol cm^{-3}).

For the sake of simplicity, the fluid flow boundary condition at the inner walls of the microchannels was defined as a no-slip condition.[20] The properties of the model fluids and relevant parameters are provided in Table S2. The initial concentrations (C_0) of the solutions from the inlets were set to be 50 mol m^{-3} and 0 mol m^{-3} for the upper (red color) and the lower inlet (blue color), respectively. As the flow rates of the two streams were identical, perfect mixing occurred when the concentration of the mixed stream was uniform and equal to 25 mol cm^{-3}. The simulation was numerically solved by the parallel sparse direct linear solver with parameters given in Table S1. Different dynamic parameters (velocity, vorticity, concentration) and Reynolds numbers of the fluid in micromixer at different channel depths (100, 200, 300, 400 μm) were compared. These parameters are associated to the flow regime that determines mixing efficiency in the micromixer.

Fabrication

A photo of the PMMA microfluidic device is presented in Fig. 1b. The channels (layer 1) and supporting plate (layer 3) were manufactured on PMMA thin sheets (1 mm thick) using a VersaLASER VLS 3.60 laser etching system (Universal Laser System). Designs of the microfluidic components were created using Corel DrawX4 (Corel Software, Ottawa, ON, Canada) interfaced directly with the CO_2 laser system. Reagents, samples and wastes were injected and removed from the device via clear acrylic tubes (ID = 4 mm) connected to the inlets and outlet, respectively. The as-prepared microelectrodes were mounted on the electrode support by epoxy adhesive. The device was sealed by a 3-mm-thick silicon joint sandwiched between the PMMA plates by four screws at the four corners.

Heterogeneous Sandwich Immunoassay in Continuous Flow Mode

Figure 2 illustrates the steps of the heterogeneous sandwich immunoassay in the microfluidic device. The biotinylated monoclonal CEA-specific antibody (Ab_1-biotin) was previously immobilized on streptavidin-coated magnetic particles through a streptavidin–biotin non-covalent bond. A rare earth magnet was placed under the working electrode. Then, the magnetic particles containing the primary antibody, antigen, and secondary antibody were injected separately into the microfluidic device. The continuous flow mode allows the removal of all unbound molecules. The use of magnetic particles enables the preconcentration of CEA in the reaction chamber, thereby increasing the probability of its detection at the microelectrode.

Electrochemical Detection of CEA

The as-prepared microfluidic system was used to detect CEA in the continuous flow mode. The magnetic beads were manipulated using an external removable magnet. The CEA antigens were allowed

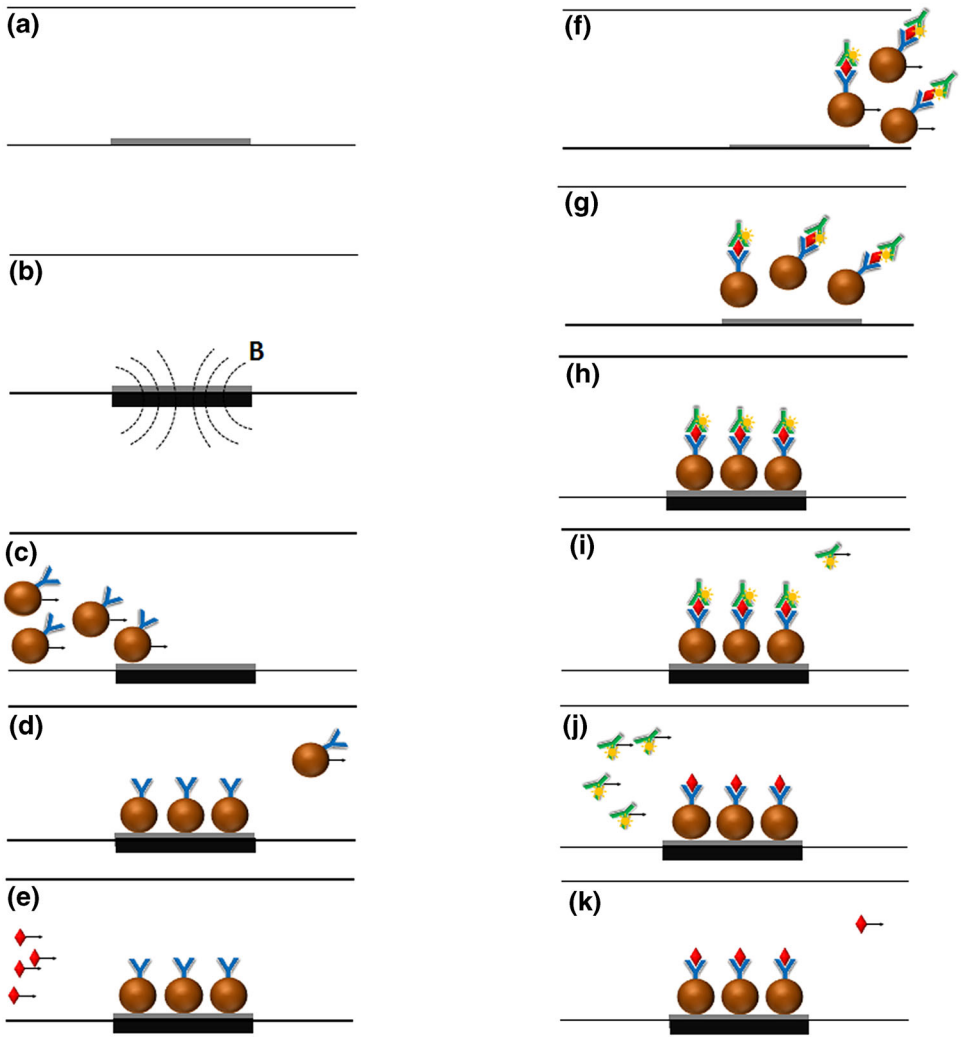

Fig. 2. The application of the device for detecting carcinoembryonic antigens in continuous flow mode: (a) bare electrode; (b) set-up an external magnetic field; (c) injection of magnetic particles (MP) containing the primary antibody (MP-Ab_1); (d) capture of MP on electrodes and washing off extra, unbound MP; (e) injection of CEA (Ag); (f) capture of CEA on electrodes and washing off unbound CEA; (g) injection of secondary antibody (Ab_2); (h) capture of secondary antibody and washing off unbound antibodies; (i) electrochemical detection of antigen/antibodies complex (MP-Ab_1-Ag-Ab_2); (j) removal of external magnetic field; and (k) washing off the antigen/antibodies complex.

to be sandwiched by two antibodies of which one was immobilized onto the magnetic particles and one was labeled with electroactive element Ru^{2+}. The capture of the antigen/antibodies complex on the sensor was recorded as electrochemical signals. Square wave voltammetry (SWV) is an excellent technique for monitoring biological binding events of immunosensor.[23] In this method, the currents were measured successively in both positive and negative pulses, and the output current was the subtraction between the oxidation and reduction peaks. Therefore, the current density was much higher than in the classic cyclic voltammetry method. Additionally, the capacitive current and parasitic current can be reduced due to the reduction of dissolved oxygen. All electrochemical measurements were performed using a handheld potentiostat DY2013 (Digi-Ivy, USA). The SWV method was conducted with the frequency of 12.5 Hz, start potential of −0.2 V, end potential of +1.1 V, step of 10 mV, and pulse amplitude of 25 mV.

RESULTS AND DISCUSSION

Numerical Simulation

The two-dimensional concentration profile of solutes at steady state in the device is presented in Fig. 3. The effectiveness of mixing was visualized by the uniform green color (25 mol cm^{-3}) at the exit. As seen in Fig. 3, when the mixer channel depth was ≤300 μm, the two streams in the device intercrossed and were well dispersed, indicating an effective mixing performance. In contrast, when the channel depth was 400 μm, the solutions from the inlets did not disperse well and flowed almost in parallel. The best mixing performance was observed in a 300-μm-deep mixer where the

most homogeneous concentration profile was obtained. Consequently, the depth of the fluidic system was fixed at 300 μm for all experiments.

In this research, velocity and vorticity profiles in the mixing zone of the fluidic system were also investigated (see Figs. 1S and 2S in the supporting information). These values were found to be much higher than in the other areas of the fluidic systems, suggesting effective mixing in the micromixer. As the mixer depth increased, the velocity and vorticity of the fluid flow became higher. The highest velocity and vorticity were 1.657 m s^{-1} and 19.687 s^{-1}, respectively (see Table I). However, it must be noted that the fast and vortex flow which enhanced mixing in the micromixer would result in turbulence in the main stream. Indeed, chaotic flow was observed at the outlet of the 400-μm-deep mixer.

The simulated results were validated by mixing two liquids (methylene blue and red dye) of different colors in the 300-μm-deep micromixer. The distribution of color during the flow was observed by naked eye and recorded by a digital camera (SX 610; Canon) (Fig.4). As expected, the mixing resulted in a uniform purple color within a few minutes, indicating complete dispersion of the dyes in the mixture. The experimental result agreed well with the simulated data. In future studies, the mixing performance might be improved by varying the mixer dimensions and geometries. Moreover, the mixer dimensions could be easily adapted to match a specific time frame regarding the mixing of the molecules.[22]

Manipulation of Magnetic Particles in Continuous Flow Mode

To enhance the reproducibility of the magnetic particle responses to the external magnetic field, the magnet needs to be aligned with the electrode. For this purpose, a custom-made PMMA holder was used to fix the position of the magnet. The manipulation of the magnetic particles is demonstrated in Fig. 3. In this approach, the magnetic particles can be easily packed, flushed and repacked in the reaction chamber by an external magnetic field. The biotinylated monoclonal CEA-specific antibody (Ab_1-biotin) was previously incubated with streptavidin-coated magnetic particles

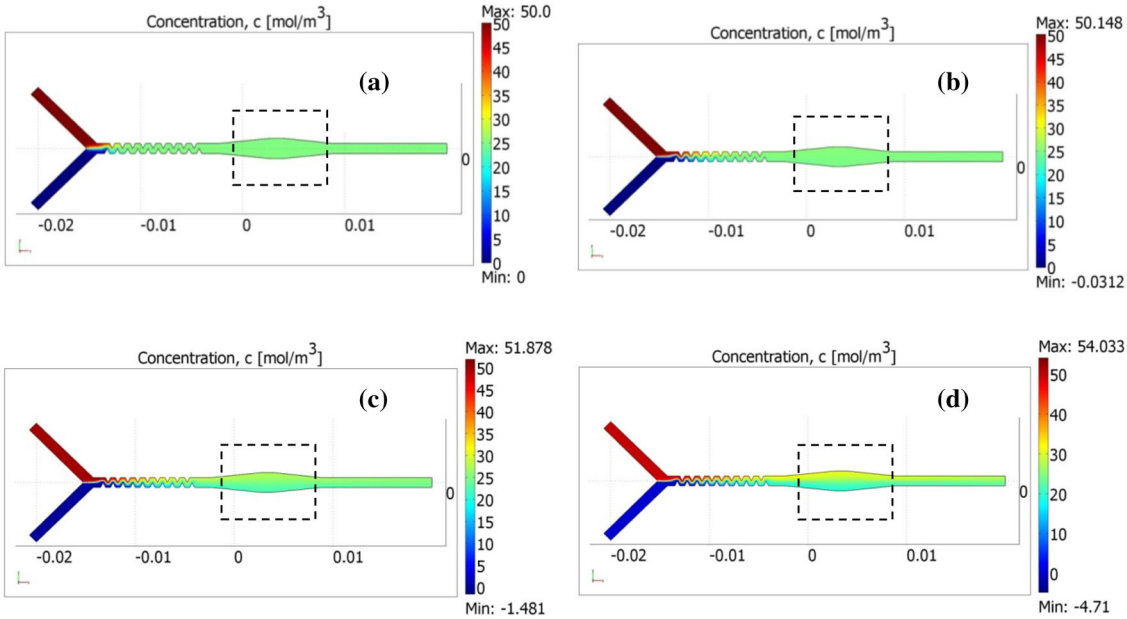

Fig. 3. Effects of channel depth on spatial distribution of concentration in the detection zone. Mixing performance of the micromixer was simulated at different channel depths: (a) 100 μm, (b) 200 μm, (c) 300 μm and (d) 400 μm. Red dye (50 mol m^{-3}) and methylene blue (50 mol m^{-3}) were separately injected in two the inlets on the left. Flow rate was fixed at 1 mL h^{-1}. Uniform mixing was indicated by green color at the outlet (a–c).

Table I. The dynamic parameters of fluid flow in the micromixer with different microchannel depths

Channel depth (μm)	Max velocity (mm s^{-1})	Max vorticity (s^{-1})	Max R_e
100	0.1331	8.547	0.0215
200	0.558	14.418	0.119
300	1.118	17.754	0.250
400	1.657	19.687	0.486

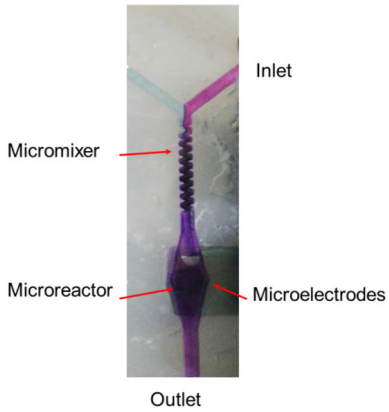

Fig. 4. Mixing performance of the device tested by two dye solutions (red dye and methylene blue A).

for 10 min. Magnetic particles immobilized with primary Ab_1 (MP-Ab_1) were collected using an external magnet and then injected into the fluidic system at a flow rate of 1 mL h^{-1}. The antigen and the secondary antibody were separately injected into the fluidic system under the same conditions. A short stop of injection flow (5 min) and a rapid wash with phosphate-buffer saline (PBS) (5 min) were performed between injection steps to ensure the removal of unbound biomolecules and the rearrangement of the magnetic particles. Finally, very high pressure was applied to remove the magnetic particles containing antigen/antibodies complexes and the fluidic device was ready for a new experiment.

The amount of magnetic particles injected into the fluidic system can be calculated by the following equations:

$$m = \left(\frac{50}{3}\right) C_0 \cdot v \cdot t \quad (1)$$

$$N = m/m_i \quad (2)$$

$$m_i = 10^{-6} \cdot \rho \cdot \left(\frac{4}{3}\right)\pi(d/2)^3 \quad (3)$$

where m (μg) is the total mass, N (particles) is the number of magnetic particles injected into the fluidic system at a velocity v (mL h^{-1}) and a concentration C_0 (mg mL^{-1}) for t (min), $m_{i\text{-}}$ (μg) is the mass of each magnetic particle with diameter d (μm), and ρ ($\sim$5 g cm^{-3}) is the mass density of the magnetic particles.

The number of particles, N_0, required to completely cover the electrode surface (100% coverage) can be estimated by:

$$N_0 = A/(\pi r^2) \quad (4)$$

where N_0 is the number of magnetic particles needed to cover the entire electrode surface, A (=π mm^2) is the area of electrode surface, and r (=1 μm) is the radius of a magnetic particle.

In this study, the diameters of the working electrode and magnetic particles were 1 mm and 1 μm, respectively. Thus, the minimal amount of magnetic particles that should be injected into fluidic devices is 1×10^6 particles. The manipulation of the magnetic particles in continuous flow mode was investigated with a flow rate from 0.1 to 10 mL h^{-1} and particle concentration of 0.72 mg mL^{-1}. Congestion of the magnetic particles was noticed if the amount of particles exceeded 50 μg, corresponding to an injection of particles at a flow rate of 0.1 mL h^{-1} for 30 min. Therefore, in all experiments, a uniform suspension of magnetic particles with a concentration of 0.72 mg mL^{-1} was injected into the fluidic devices for 10 min at a flow rate of 1 mL h^{-1}. Under these conditions, a plug of magnetic particles particles (about 12 μg, 4.6×10^6 particles $\sim 5N_0$) was packed in the reaction chamber. The flow rate was set as low as possible to facilitate uniform accumulation of the magnetic particles in the reaction chamber. In addition, the suspension of magnetic particles was sonicated for several minutes to improve the dispersion prior to the experiment.

Electrochemical Detection of CEA

The square wave voltammograms of the biological complex at different CEA concentrations are presented in Fig. 5. When a monoclonal anti-CEA antibody labeled with a ruthenium complex (Ab_2-Ru^{2+}) was introduced to the microelectrodes, a broad oxidation peak associated with Ru^{2+} was observed at +720 mV.[24] As mentioned above, the continuous flow mode allowed us to remove unbound reagents (including Ru^{2+}) from the detection chamber. Therefore, the occurrence of the oxidation peak on the SWV curves evidenced the formation of a sandwich complex containing the labeled antibody, target antigen and captured antibody. Electrochemical behavior of CEA was tested at different concentrations (4 ng mL^{-1}, 8 ng mL^{-1}, 15 ng mL^{-1}, 20 ng mL^{-1}, and 34 ng mL^{-1}) and the intensity of the Ru^{2+} peak was found to increase with the oncentration of CEA (Fig. 5).

The specificity of the developed method was also verified with using thyroid stimulating hormone (TSH) and SEB as negative samples (Fig. 5a). As seen from the data, no significant response of the current to addition of THS and SEB was recorded. The limit of detection was estimated to be 150 pg mL^{-1} which was comparable with previously reported values (see Table II).[6–12]

The total time required for each immuno-test was $<$20 min. Therefore, the proposed method could be a viable choice for detecting CEA tumor markers in clinical laboratories. However, the high CEA level might be due to either cancer or other reasons (i.e. smoking).[25] It was recently reported that

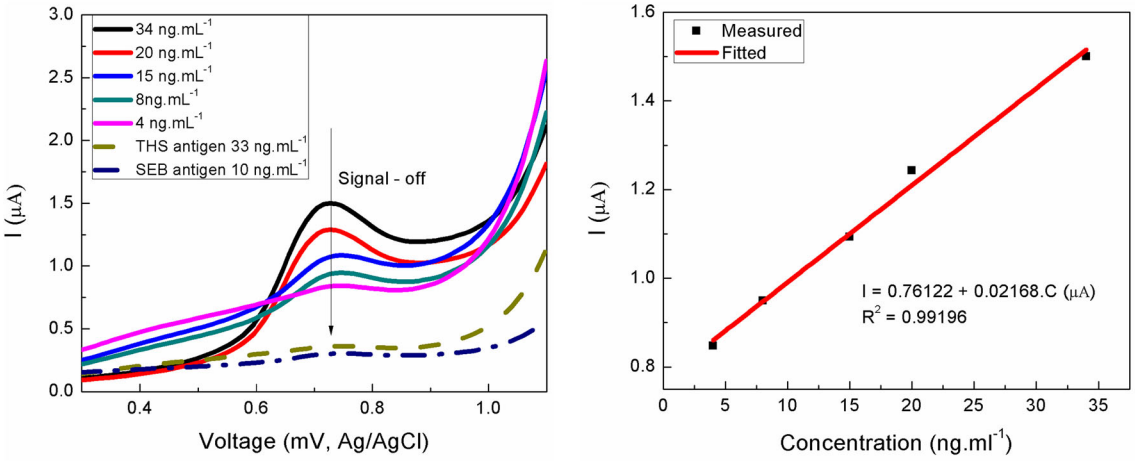

Fig. 5. Square wave voltammetry detection of CEA markers: (a) responses of current signals to CEA antigen concentrations (4–34 ng mL^{-1}); (b) correlation between CEA antigen concentration and peak currents.

Table II. Comparison of CEA detection limits by different methods and electrodes

Configuration	Combined with magnetic particles	Combined with microfluidics	Detection limit (pg mL^{-1})	References
Au-OAP	No	No	100	7
Au/CS membrane	Yes	No	220	6
Pt	Yes	Yes	150	Present work
Au/CS/Au/GCE	No	No	60	8
Au	Yes	No	1	11
PEI/MWCNT/SPE	No	No	1	10
Cu@Ag-CD-GN	No	No	0.02	12

CS chitosan, *OAP* o-aminophenol, *GCE* glassy carbon electrode, *PEI* polyethyleneimine, *MWCNT* multi-wall carbon nanotubes, *SPE* screen-printed electrodes, *CD* cyclodextrin, *GN* graphene nanosheet.

false-positive CEA level elevations in the range of 5 to 35 ng mL^{-1} might occur in some cases.[26] Therefore, diagnostic imaging studies and/or biopsy should be combined with CEA blood tests for diagnosis, staging and treatment monitoring of cancer.

CONCLUSION

In the present work, a microfluidic device based on a continuous flow immunoassay was developed for CEA detection. This approach was found to be apparently advantageous over the traditional immunoassays since it required less immunoreagents and samples (several μl), shorter analysis time (20 min), and had less non-specific adsorption of biomolecules and higher reproducibility. An additional advantage of the method was the controllable uptake/release of biomolecules which enabled the automation of biomedical analysis. The developed sensing method was also very versatile and could be applicable to other biomolecules apart from tumor markers.

ACKNOWLEDGEMENTS

Funding of this work was mainly provided by the National Foundation for Science and Technology Development (NAFOSTED) 103.02-2012.71 (Nguyen Van Anh). The authors also acknowledged the financial support from the Vietnam Academy of Science and Technology (VAST03.01/15-16). The authors are very grateful for the scientific support from Professor. Elizabeth DUFOUR-GERGAM from University Paris-Sud 11 (Paris, France).

ELECTRONIC SUPPLEMENTARY MATERIAL

The online version of this article (doi: 10.1007/s11664-016-4372-1) contains supplementary material, which is available to authorized users.

REFERENCES

1. P. Gold and S.O. Freedman, *J. Exp. Med.* 121, 439 (1965).
2. M. Uehara, T. Kinoshita, T. Hojo, T.S. Akashi, E. Iwamoto, and T. Fukutomi, *Int. J. Clin. Oncol.* 13, 447 (2008).
3. M. Grunnet and J.B. Sorensen, *Lung Cancer* 76, 138 (2012).
4. M.J. Duffy, *Clin. Chem.* 47, 624 (2001).
5. W.G. Doos, W.I. Wolff, H. Shiny, A. Dechabon, R.J. Stenger, L.S. Gottlieb, and N. Zamcheck, *Cancer* 36, 1996 (1975).
6. J. Wu, J. Tang, Z. Dai, F. Yan, H. Ju, and N.E. Murr, *Biosens. Bioelectron.* 22, 102 (2006).
7. H. Tang, J. Chen, L. Nie, Y. Kuang, and S. Yao, *Biosens. Bioelectron.* 22, 1061 (2007).
8. X. He, R. Yuan, Y. Chai, and Y. Shi, *J. Biochem. Biophys. Meth.* 70, 823 (2008).
9. B.V. Chikkaveeraiah, A.A. Bhirde, N.Y. Morgan, H.S. Eden, and X. Chen, *ACS Nano* 6, 6546 (2012).
10. S. Viswanathan, C. Rani, A.V. Anand, and J.A. Ho, *Biosens. Bioelectron.* 24, 1984 (2009).
11. Z. Altintas, S.S. Kallempudi, U. Sezerman, and Y. Gurbuz, *Sens. Actuators B: Chem.* 174, 187 (2012).
12. J. Gao, Z. Guo, F. Su, L. Gao, X. Pang, W. Cao, B. Du, and Q. Wei, *Biosens. Bioelectron.* 63, 465 (2015).
13. M.A. Hayes, T.N. Polson, A.N. Phayre, and A.A. Garcia, *Anal. Chem.* 73, 5896 (2001).
14. J.W. Choi, K.W. Oh, J.H. Thomas, W.R. Heineman, H.B. Halsall, J.H. Nevin, A.J. Helmicki, H.T. Henderson, and C.H. Ahn, *Lab Chip* 2, 27 (2002).
15. D.J. Harrison, A. Manz, Z. Fan, H. Luedi, and H.M. Widmer, *Anal. Chem.* 64, 1926 (1992).
16. G.M. Whitesides, *Nature* 442, 368 (2006).
17. J. Verbarg, K. Kamgar-Parsi, A.R. Shields, P.B. Howell, and S.L. Frances, *Lab Chip* 12, 1793 (2012).
18. F. Berti, S. Laschi, I. Palchetti, J.S. Rossier, F. Reymond, M. Mascini, and G. Marrazza, *Talanta* 77, 971 (2009).
19. K. Choi, A.H. Ng, R. Fobel, D.A. Chang-Yen, L.E. Yarnell, E.L. Pearson, C.M. Oleksak, A.T. Fischer, R.P. Luoma, J.M. Robinson, J. Audet, and A.R. Wheeler, *Anal. Chem.* 85, 9638 (2013).
20. D.L. Tran, T.D. Nguyen, H.B. Nguyen, P.Q. Do, and L.H. Nguyen, *Talanta* 85, 1560–1565 (2011).
21. V. Hessel, H. Löwe, and F. Schönfeld, *Chem. Eng. Sci.* 60, 2479 (2005).
22. T.T. Veenstra, T.S.J. Lammerink, M.C. Elwenspoek, and A. van den Berg, *J. Micromech. Microeng.* 9, 199–202 (1999).
23. A. Chen and B. Shaha, *Anal. Methods* 5, 2158 (2013).
24. E.Eskelinen and M. Haukka, *J. Chem. Soc. Dalton Trans.* 16, 2745 (2000).
25. K.M. Sajid, K. Chaouachi, and R. Mahmood, *Harm. Reduct. J.* 5, 19 (2008).
26. A. Litvak, A. Cercek, N. Segal, D. Reidy-Lagunes, Z.K. Stadler, R.D. Yaeger, N.E. Kemeny, M.R. Weiser, M.S. Pessin, and L. Saltz, *J. Natl. Compr. Canc. Netw.* 12, 907 (2014).